Int. J. Electrochem. Sci., 10 **(2015)** 6651 - 6662

International Journal of
ELECTROCHEMICAL
SCIENCE
www.electrochemsci.org

Facile synthesis of high performance $LiNi_{0.5}Mn_{1.4}Mg_{0.1}O_4$ and $LiNi_{0.5}Mn_{1.4}Al_{0.1}O_4$ by a low temperature solution combustion synthesis method

Guiyang Liu [1, 2, *], *Hongyan Sun*[1, 2], *Xin Kong*[1, 2], *Yannan Li* [1, 2], *Baosen Wang* [1, 2]

[1] Lab of New Materials for Power Sources, College of Science, Honghe University, Mengzi 661199, Yunnan, China.
[2] Local Characteristic Resource Utilization and New Materials Key Laboratory of Universities in Yunnan, Honghe University, Mengzi 661199, Yunan, China.
[*]E-mail: liuguiyang@tsinghua.org.cn

Received: 15 April 2015 / *Accepted:* 28 May 2015 / *Published:* 24 June 2015

$LiNi_{0.5}Mn_{1.4}Mg_{0.1}O_4$ and $LiNi_{0.5}Mn_{1.4}Al_{0.1}O_4$ was synthesized by a low temperature solution combustion synthesis method at 700 ◦C in 30 min. Both of the two products are non-stoichiometric and disordered $LiNi_{0.5}Mn_{1.5}O_4$ spinels. The two products exhibit similar reversible capacity and excellent cycling stability at 1C rate at room temperature. The initial reversible capacity of $LiNi_{0.5}Mn_{1.4}Mg_{0.1}O_4$ and $LiNi_{0.5}Mn_{1.4}Al_{0.1}O_4$ are 114 mAh/g and 113 mAh/g, and remain 100.0% and 98.9% after 100 cycles at 1C, respectively. $LiNi_{0.5}Mn_{1.4}Mg_{0.1}O_4$ shows better rate capability and much better cycling stability at 10C rate than these of $LiNi_{0.5}Mn_{1.4}Al_{0.1}O_4$. At 10C rate, the capacity retention of $LiNi_{0.5}Mn_{1.}4Mg_{0.1}O_4$ is near 100% after 100 cycles, but the capacity retention of $LiNi_{0.5}Mn_{1.4}Al_{0.1}O_4$ is only 80%. $LiNi_{0.5}Mn_{1.4}Mg_{0.1}O_4$ also displays better cycling stability at 55 ^oC than that of $LiNi_{0.5}Mn_{1.4}Al_{0.1}O_4$. The excellent electrochemical performance of $LiNi_{0.5}Mn_{1.4}Mg_{0.1}O_4$ is attributed to its higher crystallinity, larger Li^+ diffusion coefficient and lower charge transfer resistance.

Keywords: Lithium ion batteries, $LiNi_{0.5}Mn_{1.5}O_4$ spinels, cathode materials, doping

1. INTRODUCTION

$LiNi_{0.5}Mn_{1.5}O_4$ spinel is one of the most promising cathode materials for lithium ion batteries because of its high operating voltage, good rate capability and low cost [1]. However, for practical applications, especially the application in electric vehicles (EVs) or hybrid electric vehicles (HEVs), the electrochemical performances of $LiNi_{0.5}Mn_{1.5}O_4$ including cycling stability especially at elevated temperatures and rate capability need to be significantly improved [2].

Doping has been proved to be one of the most efficient routes to improve the electrochemical performance of $LiNi_{0.5}Mn_{1.5}O_4$ [3, 4]. In the literatures, $LiNi_{0.5}Mn_{1.5}O_4$ spinels doped by Mg [5], Al [6], Ti [7], Ga [8] and W [9] have been reported and exhibit improved electrochemical performance. Among them, Mg and Al are more attractive because of their light weight and high efficiency for improving the performance of $LiNi_{0.5}Mn_{1.5}O_4$ [10-12].

For the preparation of doped $LiNi_{0.5}Mn_{1.5}O_4$, it is important that the raw materials must be mixed homogeneously. Different synthesis methods such as solid-state method [13], sol-gel method [14] or co-precipitation synthesis [15] producing doped $LiNi_{0.5}Mn_{1.5}O_4$ with different electrochemical performance have been reported. Although solid-state method is the simplest, the mixture of raw materials is non-homogeneous. In order to prepare single phase doped $LiNi_{0.5}Mn_{1.5}O_4$, high temperature and long time are needed. However, high temperature generally results in increased grain size and impurities such as $Li_xNi_{1-x}O$ in the final product, leading to rate capability declining and capacity fading [16]. Other methods such as sol-gel method and co-precipitation method can obtain homogenous precursors and the electrochemical performance of the products can be improved, but the processes of them are complicated, resulting in the limitation in practical manufacturing applications.

Solution combustion synthesis method is a simple method to synthesize metal oxides at low temperature [17]. Due to the ionic level's mixture of the raw materials in solution, doping could be easily carried out. In this paper, we introduced a modified low temperature solution combustion synthesis method to prepare Al and Mg doped $LiNi_{0.5}Mn_{1.5}O_4$. Based on the optimization of the experimental conditions of the improved solution combustion synthesis method [18, 19], doped $LiNi_{0.5}Mn_{1.5}O_4$ spinels with excellent electrochemical performance could be synthesized at 700^{o}C in only 30 min. The total process took no more than 1 h. Although Mg and Al doping in $LiNi_{0.5}Mn_{1.5}O_4$ synthesized by other methods have been widely reported, to our knowledge, it has not been reported that Mg and Al doped $LiNi_{0.5}Mn_{1.5}O_4$ spinels with such excellent performance could be synthesized in such a short time. The electrochemical performances including capacity, cycling stability, rate capability of the products have been studied in details.

2. EXPERIMENTAL

2.1 Synthesis

For the synthesis of $LiNi_{0.5}Mn_{1.4}Mg0.1O_4$ (or $LiNi_{0.5}Mn_{1.4}Al0.1O_4$), raw materials of $LiNO_3$, CH_3COOLi, $Mn(NO_3)_2$, $(CH_3COO)_2Mn$, $Ni(NO_3)_2$, $(CH_3COO)_2Ni$ and $Mg(NO_3)_2$ (or $Al(NO_3)_3$) (AR, 99%, Aladdin) with the mole ratio of 0.5:0.5:0.7:0.7:0.25:0.25:0.1 were firstly dissolved in distilled water to obtain a solution. Then, the solution was combusted in a muffle furnace preset at 700°C directly for 30 minutes. And then the product was taken out and cooled down to room temperature in air. The final $LiNi_{0.5}Mn_{1.4}Mg_{0.1}O_4$ (or $LiNi_{0.5}Mn_{1.4}Al_{0.1}O_4$) was obtained.

2.2 Phase composition and morphology

The phase composition and structure of the products were determined by X-ray diffraction (XRD, D/max-rB, Cu-Kα radiation) and Fourier transform infrared spectroscopy (FTIR, Perkin Elmer, with KBr pellets). The morphologies of the products were observed by scanning electron microscope (SEM, XL30ESEM-TMP, Philips).

2.3 Elctrochemical performance test

The electrochemical performance of the as-prepared $LiNi_{0.5}Mn_{1.5}O_4$ powders was tested in a standard CR2032 coin cell, which was composed of a cathode, lithium anode, a Celgard polypropylene separator, and LiPF6 in 1:1 ethylene carbonate/diethylene carbonate (EC/DEC) as electrolyte. The chathode electrode was composed of 80 wt.% active material, 12 wt.% conductive carbon, and 8 wt.% polyvinylidene fluoride binder. The cells were assembled in an argon-filled glove box and cycled at room temperature and 55 ^{o}C in the voltage ranege of 3.5 - 5.0V (versus Li/Li^+) at different C rate (in this paper, 1C=150mA/g). Cyclic voltammograms (CV) and electrochemical impedance spectroscopy (EIS) of the products were carried out by an electrochemical workstation (Autolab PGSTAT302N, Metrohm, Switzerland). The scan rate was from 0.1 to 0.5 mV/s between 3.5-5.0 V, and the frequency range was 10 kHz to 0.1 Hz with an AC amplitude of 5 mV. Before EIS test, the cell was charged to 5V at 100% state.

3. RESULTS AND DISCUSSION

3.1 Phase structure and micro-morphologies

XRD patterns of the products were shown in Fig.1. It can be seen that all peaks of the products correspond to $LiNi_{0.5}Mn_{1.5}O_4$ (JCPDS 80-2162) and no evident other peaks appeared, suggesting that single phase $LiNi_{0.5}Mn_{1.5}O_4$ spinels were obtained. Because of the larger ionic radius of Mg^{2+} than that of Al^{3+} [20, 21], the calculated lattice parameter of $LiNi_{0.5}Mn_{1.4}Mg_{0.1}O_4$ is 0.81939 nm, larger than 0.81784nm of the $LiNi_{0.5}Mn_{1.4}Al_{0.1}O_4$. Because the ionic radius of Al^{3+} is smaller than that of Mn^{3+} [21], the lattice parameter of the $LiNi_{0.5}Mn_{1.4}Al_{0.1}O_4$ should be smaller than 0.817nm of the standard pristine $LiNi_{0.5}Mn_{1.5}O_4$. However, the calculated lattice parameter of the $LiNi_{0.5}Mn_{1.4}Al_{0.1}O_4$ is larger, suggesting that the as-prepared Al^{3+} doped $LiNi_{0.5}Mn_{1.5}O_4$ spinel is non-stoichiometric and disordered [22]. There are two types of $LiNi_{0.5}Mn_{1.5}O_4$ spinel, disordered Fd_3m or ordered $P4_332$ [4]. In the stoichiometric and ordered $LiNi_{0.5}Mn_{1.5}O_4$ spinel, Ni^{2+} and Mn^{4+} ions exhibit a cation site ordering over two distinct octahedral positions at 4a and 16d sites, respectively [6]. For the non-stoichiometric $LiNi_{0.5}Mn_{1.5}O_{4-\delta}$, because of the loss of oxygen, part of the inactive Mn^{4+} ions would be reduced to Mn^{3+} to keep charge neutrality. Becuase the ionic radius of Mn^{3+} is larger than that of Mn^{4+}, the lattice parameters of the non-stoichiometric $LiNi_{0.5}Mn_{1.5}O_{4-\delta}$ generally increase with increasing Mn^{3+} in the lattice [23].

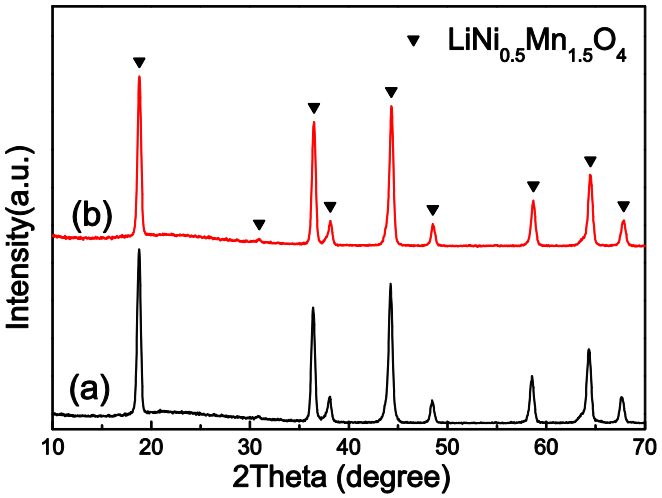

Figure 1. XRD patterns of (a) $LiNi_{0.5}Mn_{1.4}Mg_{0.1}O_4$ and (b) $LiNi_{0.5}Mn_{1.4}Al_{0.1}O_4$.

The cation ordering of $LiNi_{0.5}Mn_{1.5}O_4$ can be determined by FT-IR spectroscopy effectively [24]. When the cation ordering of $LiNi_{0.5}Mn_{1.5}O_4$ increases, the intensity of Ni–O band at 588 cm^{-1} will increase and the intensity of Mn–O band at 620 cm^{-1} will decrease [25]. For example, a typical highly ordered structure shows a higher intensity of Ni–O band at about 588 cm^{-1} than that of Mn–O band at 620 cm^{-1} [26]. As shown in Fig.2, the band intensity of all the products at 585 cm^{-1} is lower than that at 620 cm^{-1}, suggesting that the two products have disordered structure with space group of Fd_3m.

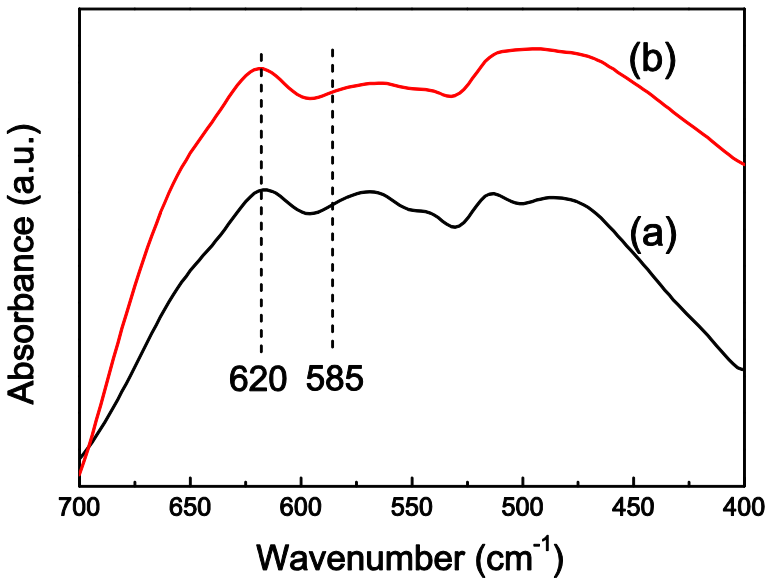

Figure 2. FT-IR spectra patterns of (a) $LiNi_{0.5}Mn_{1.4}Mg_{0.1}O_4$ and (b) $LiNi_{0.5}Mn_{1.4}Al_{0.1}O_4$.

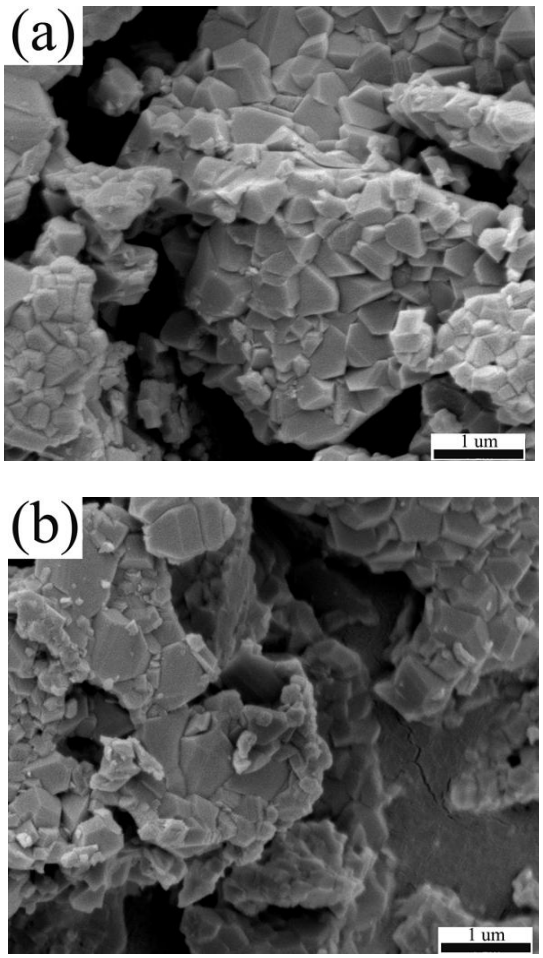

Figure 3. SEM images of (a) $LiNi_{0.5}Mn_{1.4}Mg_{0.1}O_4$ and (b) $LiNi_{0.5}Mn_{1.4}Al_{0.1}O_4$.

The SEM micro morphologies of the products are shown in Fig.3. It can be found that the micro morphologies of $LiNi_{0.5}Mn_{1.4}Mg_{0.1}O_4$ (as shown in Fig.3a) exhibit developed grains with ~300-500nm in size. The surface facets are very clear, indicating that the sample is well crystallized. Differently, besides developed grains, $LiNi_{0.5}Mn_{1.4}Al_{0.1}O_4$ also shows lots of small agglomerated particles, as shown in Fig.3b. From the small particles, typical octahedral surface facets of the spinel cannot be found, suggesting that some grains of $LiNi_{0.5}Mn_{1.4}Al_{0.1}O_4$ are not well developed.

3.2 Electrochemical performance

The initial charge/discharge curves of the $LiNi_{0.5}Mn_{1.4}Mg_{0.1}O_4$ and $LiNi_{0.5}Mn_{1.4}Al_{0.1}O_4$ are shown in Fig.4a. There are two voltage plateaus the curves. The main plateau at 4.7 V is attributed to Ni^{4+}/Ni^{3+} and Ni^{3+}/Ni^{2+} redox reactions, and the minor plateau at 4.0 V is ascribed to the redox reaction between the Mn^{3+} and Mn^{4+} couple [27]. The initial discharge capacities from the products of $LiNi_{0.5}Mn_{1.4}Mg_{0.1}O_4$ and $LiNi_{0.5}Mn_{1.4}Al_{0.1}O_4$ are around 114 mAh/g and 113 mAh/g, respectively. The capacity contribution from the 4.0 V plateau could be calculated from the capacity between 3.80 and 4.25 V, which could qualitatively reflect the relative concentration of Mn^{3+} ions in the spinels [22].

The calculated capacities from 4.0V of $LiNi_{0.5}Mn_{1.4}Mg_{0.1}O_4$ and $LiNi_{0.5}Mn_{1.4}Al_{0.1}O_4$ are 27 and 28 mAh/g, respectively. The considerable capacities from 4.0V plateaus of the products reveal that there are considerable Mn^{3+} ions in the products, and also indicate that the products are non-stoichiometric and disordered, which can support the results of XRD and FT-IR.

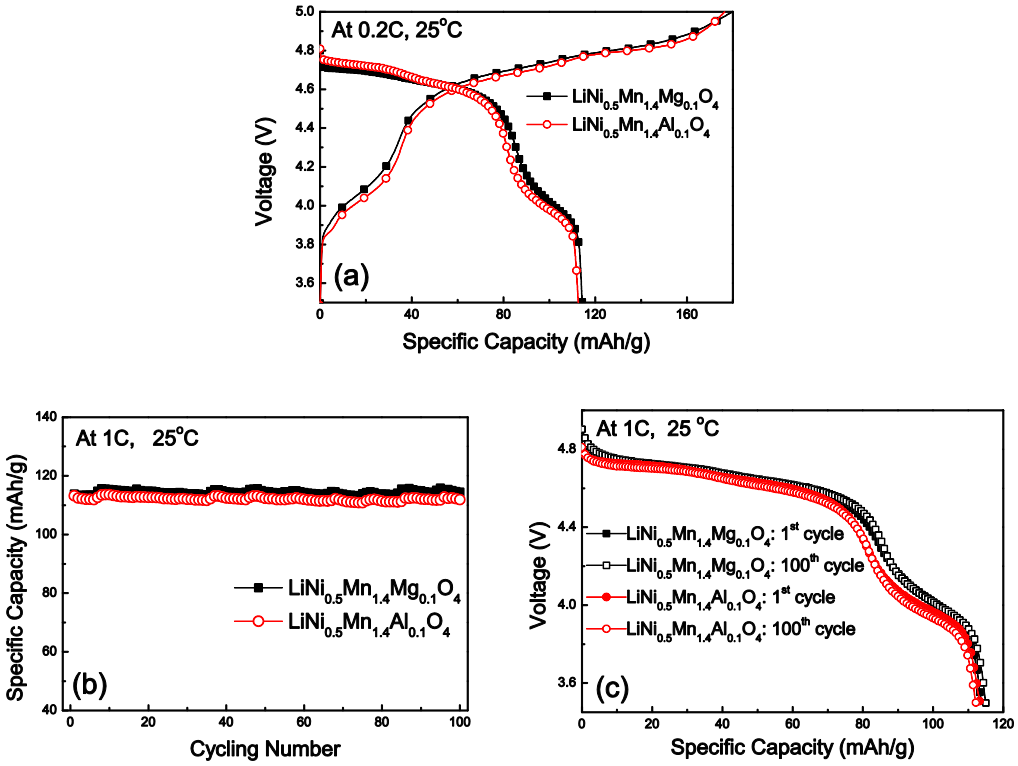

Figure 4. (a) Initial charge/discharge curves of the products. The cell was firstly charged to 5.0 V at 0.2C and held for 10min at 5.0 V, and then discharged to 3.5 V at 0.2C. (b) Cycling stabilities of the products. The cell was charged at 0.5C and discharged at 1C in 3.5-5.0V. (c) The discharge curves of the products of the 1^{st} cycle and the 100^{th} cycle.

Fig.4b shows the cycling performances of the products. The capacity retentions of $LiNi_{0.5}Mn_{1.4}Mg_{0.1}O_4$ and $LiNi_{0.5}Mn_{1.4}Al_{0.1}O_4$ after 100 cycles are 100.0% and 98.9%, respectively. Both the products exhibit excellent cycling stabilities, especially the Mg^{2+} doped one. Moreover, after 100 cycles at 1C discharge rate, the plateau voltage in the discharge curve of the two products change little (Fig.4c), also suggesting the stable cycling performance of the products. Noticeably, the calcination temperature and time of the products are only 700°C and 30min. To our knowledge, no reported $LiNi_{0.5}Mn_{1.5}O_4$ could possess such high capacity retention in such short synthesis time. Compared with the doped $LiNi_{0.5}Mn_{1.5}O_4$ prepared by co-deposition method [5], sol-gel method [10] or self-sacrifice template method [26], the capacity retentions of the as-prepared products in this paper are also superior. Zhong [6], Lafont [10] and Ooms [28] reported that Mg and Al doping can stabilize

the host structure against repeated de-intercalation of the Li^+ ion therefore can enhance the cycling stability of the $LiNi_{0.5}Mn_{1.5}O_4$.

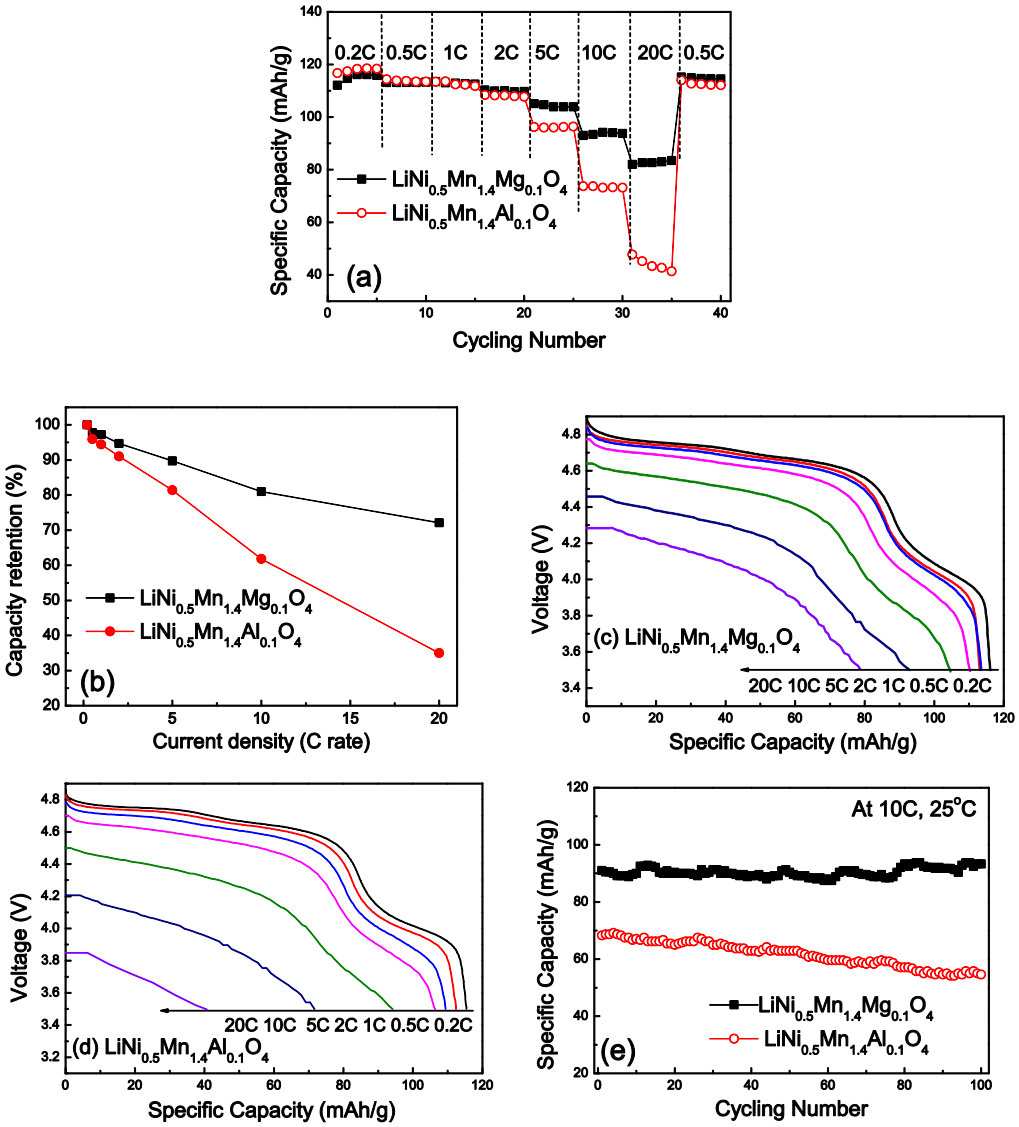

Figure 5. (a) Rates capabilitis of the products. (b) Capacity retentions at different rates of the products. (c) Charge/discharge curves of $LiNi_{0.5}Mn_{1.4}Mg_{0.1}O_4$ at different rate. (d) Charge/discharge curves of $LiNi_{0.5}Mn_{1.4}Al_{0.1}O_4$ at different rate. (e) Cycling performance of the products at 10C rate. The cell was charged at a slow rate of 0.5C when discharge rate is ≥ 0.5C.

Fig.5 shows the rate capabilities of the products. The product $LiNi_{0.5}Mn_{1.4}Mg_{0.1}O_4$ shows excellent capacity retention with increasing C rate (as seen in Fig.5a). Even at a high rate of 20C, the capacity of $LiNi_{0.5}Mn_{1.4}Mg_{0.1}O_4$ is also 84 mAh/g. However, for $LiNi_{0.5}Mn_{1.4}Al_{0.1}O_4$, at 5C, the capacity appears an obvious drop, and at 20C, the capacity becomes only about 40 mAh/g. The capacity retentions at different C rate relative to the capacity at 0.2C are shown in Fig.5b. It can be seen from Fig.5b that the capacity retention of $LiNi_{0.5}Mn_{1.4}Mg_{0.1}O_4$ is much better than that of $LiNi_{0.5}Mn_{1.4}Al_{0.1}O_4$.

It can be seen from Fig.5c and Fig.5d that the polarizations from 0.2C to 2C of the two products are small, revealing that at lower rate, the two products show good rate capabilities. However, when the rate is above 5C, the voltage drop of $LiNi_{0.5}Mn_{1.4}Al_{0.1}O_4$ is larger than that of $LiNi_{0.5}Mn_{1.4}Mg_{0.1}O_4$. At 20C, $LiNi_{0.5}Mn_{1.4}Mg_{0.1}O_4$ still maintains an operation voltage close to 4.2V. Contrastively, the operation voltage of $LiNi_{0.5}Mn_{1.4}Al_{0.1}O_4$ badly drops to 3.7V. $LiNi_{0.5}Mn_{1.4}Mg_{0.1}O_4$ shows smaller polarization with increasing C rate.

$LiNi_{0.5}Mn_{1.4}Mg_{0.1}O_4$ displays much better cycle stability than that of $LiNi_{0.5}Mn_{1.4}Al_{0.1}O_4$. As shown in Fig.5e, the capacity retentions of $LiNi_{0.5}Mn_{1.4}Mg_{0.1}O_4$ are near 100%, but the capacity retention of $LiNi_{0.5}Mn_{1.4}Al_{0.1}O_4$ is only 80% at 10C rate after 100 cycles. Mg doping is more efficient for improving the rate capability of $LiNi_{0.5}Mn_{1.5}O_4$ than Al doping. Moreover, because the two products are non-stoichiometric and disordered, and the presence of oxygen defect and Mn^{3+} ions in the two products could improve their rate capabilities [22, 24, 29], the as-prepared $LiNi_{0.5}Mn_{1.4}Al_{0.1}O_4$ and $LiNi_{0.5}Mn_{1.4}Mg_{0.1}O_4$ exhibit better rate capabilities than many previously reported $LiNi_{0.5}Mn_{1.5}O_4$ spinels [30, 31].

Voltammetry measurements of $LiNi_{0.5}Mn_{1.4}Mg_{0.1}O_4$ and $LiNi_{0.5}Mn_{1.4}Al_{0.1}O_4$ were performed to further study the electrochemical performance. Fig.6a and Fig.6b show the cyclic voltammograms (CVs) of $LiNi_{0.5}Mn_{1.4}Mg_{0.1}O_4$ and $LiNi_{0.5}Mn_{1.4}Al_{0.1}O_4$ scanned from 0.1 to 0.5mV/s, respectively. two regions at 4.0V and 4.7V appear in the CVs. The two redox pairs in 4.0V regions of the products are evident, suggesting the existence of the Mn^{4+}/Mn^{3+} couple in the products, which confirm the results of charge/discharge curves. When the scan rates increase from 0.1 to 0.5 mV/s, the change of voltage gaps between each redox couple of $LiNi_{0.5}Mn_{1.4}Mg_{0.1}O_4$ is smaller than that of $LiNi_{0.5}Mn_{1.4}Al_{0.1}O_4$. It suggests that the polarization of $LiNi_{0.5}Mn_{1.4}Mg_{0.1}O_4$ is smaller than that of $LiNi_{0.5}Mn_{1.4}Al_{0.1}O_4$.

Fig.6a and Fig.6b also show that as the scanning rate (v) is increased, the peak current (i_p) increases. Fig.6c shows the i_p vs. the square root of the scan rates ($v^{1/2}$) of the products. All of them display linear increase, which suggests that the intercalation reaction is a solid-state diffusion controlled reaction [32]. Moreover, the diffusion coefficient of Li^+ (D_{Li}) can be approximately determined by the dependence of i_p on $v^{1/2}$ based on the following equation [33]:

$$i_p = 2.69\times10^5 n^{\frac{3}{2}} A C_{Li} D_{Li}^{\frac{1}{2}} \upsilon^{\frac{1}{2}} \qquad (1)$$

Where n is the number of electrons per reaction species (for lithium-ion n=1), A is the total surface area of the electrode (2 cm^2 in this case), and C_{Li} is the bulk concentration of Li^+ in the electrode (given as 0.02378 mol/cm^3) [34, 35]. From the slope of linear fit of $\mathbf{i_p}$ vs. $\mathbf{v^{1/2}}$ in Fig.6d, the diffusion coefficients (D_{Li}) of $LiNi_{0.5}Mn_{1.4}Mg_{0.1}O_4$ and $LiNi_{0.5}Mn_{1.4}Al_{0.1}O_4$ have been calculated as $5.30\times10^{-12}cm^2/s$ and $2.00\times10^{-12}cm^2/s$ respectively. The calculated D_{Li} values are in accord with to the values reported previously [36, 37]. It has been reported that disordered (Fd_3m) $LiNi_{0.5}Mn_{1.5}O_4$ shows 1-2 order of magnitude larger D_{Li} than ordered $LiNi_{0.5}Mn_{1.5}O_4$ ($P4_332$) [38]. The calculated D_{Li} values of our products are 1-2 order of magnitude higher than those ordered $LiNi_{0.5}Mn_{1.5}O_4$ reported previously, suggesting that the phase structure of the products are disordered structure. The result is in agreement with the analysis of FTIR above. D_{Li} is an important factor for improving the rate capability

[36], the larger D_{Li} of $LiNi_{0.5}Mn_{1.4}Mg_{0.1}O_4$ results in better rate capability than that of $LiNi_{0.5}Mn_{1.4}Al_{0.1}O_4$. Theoretically, the bond strength of Al-O is stronger than these of Mg-O [21], which may results in more difficult lithium ion diffusion in the lattice, therefore leads to the larger D_{Li}.

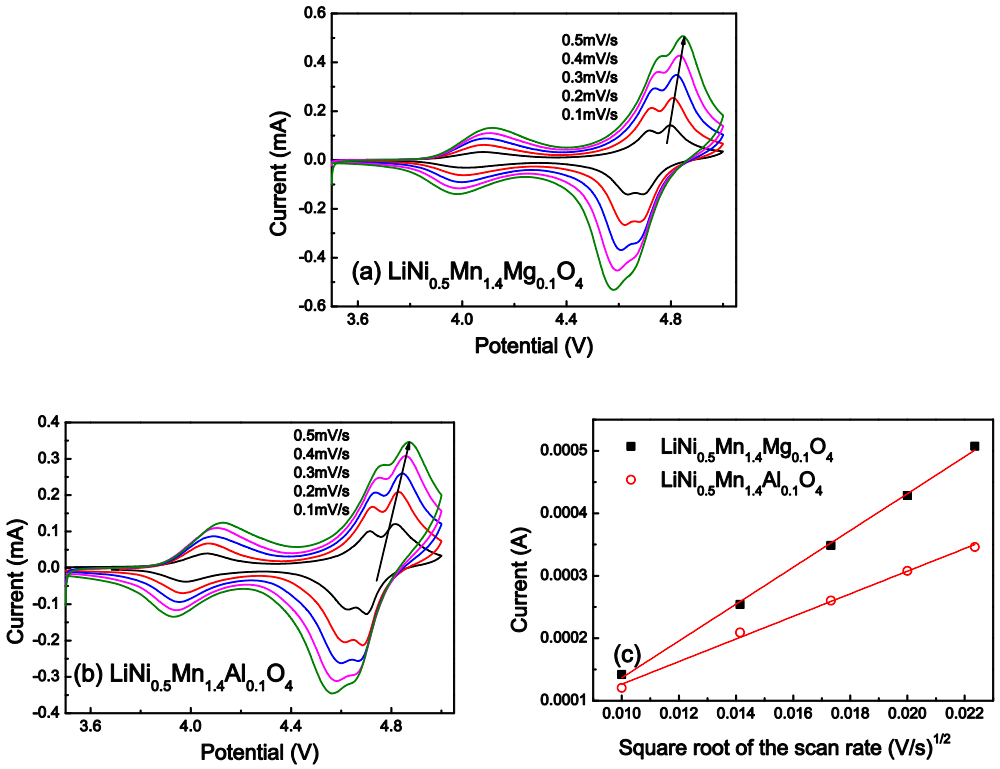

Figure 6. Cyclic voltammogram (CV) of (a) $LiNi_{0.5}Mn_{1.4}Mg_{0.1}O_4$ and (b) $LiNi_{0.5}Mn_{1.4}Al_{0.1}O_4$ at different scan rate. (c) The plotting of peak current vs. square root of the scan rate for the products.

The EIS of the cell with $LiNi_{0.5}Mn_{1.4}Mg_{0.1}O_4$ and $LiNi_{0.5}Mn_{1.4}Al_{0.1}O_4$ as electrodes are shown in Fig.7. The EIS spectrums consist of two semicircles in high-to-medium frequency region and an inclined line in low frequency region. The two semicircles are lithium-ion migration resistance (R_f) and the charge transfer resistance (R_{ct}), respectively, and the inclined line in the low frequency region is the Warburg impedance of solid phase diffusion (σ_w) [39-41]. Apparently, it can be seen from Fig.7 that the R_{ct} of $LiNi_{0.5}Mn_{1.4}Mg_{0.1}O_4$ is lower than that of $LiNi_{0.5}Mn_{1.4}Al_{0.1}O_4$. Lower R_{ct} value of $LiNi_{0.5}Mn_{1.5}O_4$ implies a lower electrochemical polarization, which leads to better rate capability [4], and higher R_{ct} means more capacity loss at the higher charge/discharge rate [41]. Combining the EIS with the CV analysis, it is clear that due to the larger D_{Li} and lower R_{ct}, $LiNi_{0.5}Mn_{1.4}Mg_{0.1}O_4$ exhibit better rate capability and better cycle stability at high rate than these of $LiNi_{0.5}Mn_{1.4}Al_{0.1}O_4$, which are in good agreement with the C-rate investigation.

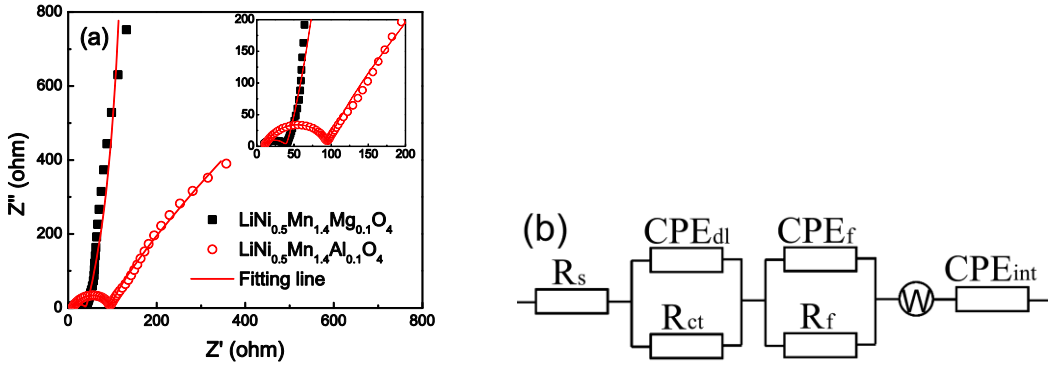

Figure 7. (a) EIS spectra of $LiNi_{0.5}Mn_{1.4}Mg_{0.1}O_4$ and $LiNi_{0.5}Mn_{1.4}Al_{0.1}O_4$ in the frequency range between 0.1 Hz and 100 kHz. (b) The equivalent circuit of the EIS.

The main drawback of the $LiNi_{0.5}Mn_{1.5}O_4$-based cathodes is the severe capacity loss when cycling is carried out at elevated temperature [42]. The cycling performances at 55 ◦C of the products are shown in Fig. 9. Although the initial capacities of the products are similar with the results at 25 ◦C, the capacity fading of the products is more obvious at 55 ◦C. The capacity retention after 100 cycles at 1C at 55 ◦C of $LiNi_{0.5}Mn_{1.4}Mg_{0.1}O_4$ is 88.6%, higher than that of 82.3% of $LiNi_{0.5}Mn_{1.4}Al_{0.1}O_4$. The higher capacity retention at 55 ◦C of $LiNi_{0.5}Mn_{1.4}Mg_{0.1}O_4$ than that of $LiNi_{0.5}Mn_{1.4}Al_{0.1}O_4$ may be attributed to the higher crystallinity of $LiNi_{0.5}Mn_{1.4}Mg_{0.1}O_4$ [43]. Although the capacity loss of the two products at 55◦C is larger than that at 25 ◦C, they are still better than many doped $LiNi_{0.5}Mn_{1.5}O_4$ spinels [6, 44].

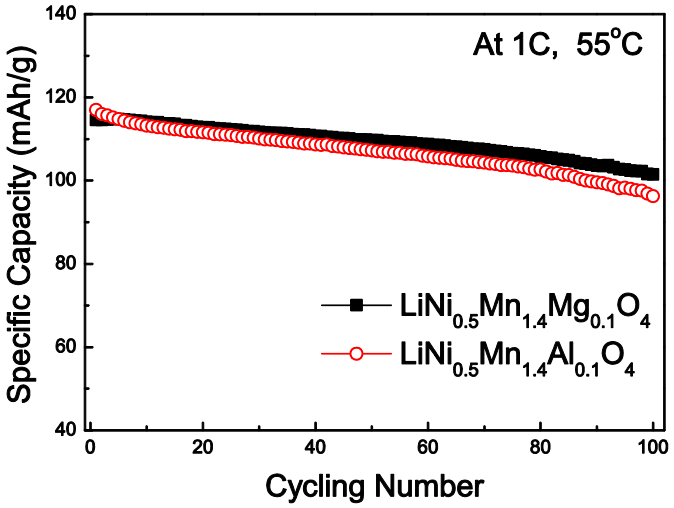

Figure 8. Cycling performance of $LiNi_{0.5}Mn_{1.4}Mg_{0.1}O_4$ and $LiNi_{0.5}Mn_{1.4}Al_{0.1}O_4$ at 55°C. The cell was charged at 0.5C and discharged at 1C at 55°C in the voltage range of 3.5-5.0V.

4. CONCLUSION

Single phase disordered $LiNi_{0.5}Mn_{1.4}Mg_{0.1}O_4$ and $LiNi_{0.5}Mn_{1.4}Al_{0.1}O_4$ were synthesized successfully by an optimized solution combustion synthesis method at 700 ◦C in only 30min. The two

products exhibit similar reversible capacity and cycling stability at 1C rate at room temperature, but $LiNi_{0.5}Mn_{1.4}Mg_{0.1}O_4$ shows better rate capability, better cyling stability at 10C rate and better elevated-temperature cycling stability than these of $LiNi_{0.5}Mn_{1.4}Al_{0.1}O_4$. $LiNi_{0.5}Mn_{1.4}Mg_{0.1}O_4$ delivers an initial reversible capacity of 114 mAh/g and remains 100.0% after 100 cycles at 1C. At 10C, the capacity is still 91 mAh/g and remains also 100.0% after 100 cycles. The excellent electrochemical performance of $LiNi_{0.5}Mn_{1.4}Mg_{0.1}O_4$ is attributed to its higher crystallinity, larger Li^+ diffusion coefficient and lower charge transfer resistance.

ACKNOWLEDGEMENT
The present work was supported by the National Natural Science Foundation of China (No. 51362012), Natural Science Foundation of Yunnan Province (2012FB173) and the Key Construction Disciplines of Chemistry for Master Degree Program in Yunnan.

Reference

1. H. Li, Z. Wang, L. Chen, X. Huang, *Adv. Mater.,* 21(2009) 4593.
2. A. Manthiram, J. Phys. *Chem. Lett.,* 2(2011) 176.
3. A. Ito, D. Li, Y. Lee, K. Kobayakawa, Y. Sato, *J. Power Sources,* 185 (2008)1429.
4. T. Yi, Y. Xie, Y. Zhu, R. Zhu, M. Ye, *J. Power Sources,* 211 (2012) 59.
5. M. Liu, H. Huang, C. Lin, J. Chen, S. Liao, *Electrochim. Acta,* 120 (2014) 133.
6. G.B. Zhong, Y.Y. Wang, Z.C. Zhang, C.H. Chen, *Electrochim. Acta,* 56 (2011) 6554.
7. J. Kim, N.P.W. Pieczonka, Y. Sun, B.R. Powell, *J. Power Sources,* 262(2014) 62.
8. D.W. Shin, A. Manthiram, *Electrochem. Commun.,* 13 (2011) 1213.
9. S.J.R. Prabakar, S.C. Han, S.P. Singh, D.K. Lee, K.S. Sohn, M. Pyo, *J. Power Sources,* 209 (2012) 57.
10. C. Locati, U. Lafont, L. Simonin, F. Oomsb, E.M. Kelder, *J. Power Sources,* 174 (2007) 847.
11. X. Wang, O. Tanaike, M. Kodama, H. Hatori, *J. Power Sources,* 168 (2007) 282.
12. G. Zhong, Y. Wang, X. Zhao, Q. Wang, Y. Yu, C. Chen, *J. Power Sources,* 216 (2012) 368.
13. H. Wang, H. Xia, M. Lai, L. Lu, *Electrochem. Commun.,* 11 (2009) 1539.
14. G. Liu, L. Zhang, L. Sun, L. Wang, *Mater. Res. Bull.,* 48 (2013) 4960.
15. J. Liu, Z. Sun, J. Xie, H. Chen, N. Wu, B. Wu, *J. Power Sources,* 240 (2013) 95.
16. H. Fang, Z. Wang, X. Li, H. Guo, W. Peng, *Mater. Lett.,* 60 (2006) 1273.
17. X. Kong, H. Sun, Q. Wang, Z. Yi, B. Wang, G. Liu, *Ceram. Int.,* 40 (2014) 11611.
18. G. Liu, X. Kong, H. Sun, B. Wang, *Ceram. Int.,* 40 (2014) 14391.
19. G. Liu, X. Kong, B. Wang, *J. Electrochem. Soc.,* 161(2014) A742.
20. R.D. Shannon, *Acta Crystallogr.,* A32(1976) 751.
21. Lide, David R., ed. CRC handbook of chemistry and physics. CRC press, 2004.
22. D. Liu, Y. Lu, J.B. Goodenough, *J. Electrochem. Soc.,* 157 (2010) A1269
23. J. Xiao, X. Chen, P.V. Sushko, M.L. Sushko, L. Kovarik, J. Feng, Z. Deng, J. Zheng, G.L. Graff, Z. Nie, D. Choi, J. Liu, J. Zhang, M. Whittingham, *Adv. Mater.,* 24 (2012) 2109.
24. G. Liu, X. Kong, H. Sun, B. Wang, Z. Yi, Q. Wang, *Electrochim. Acta,* 141 (2014) 141.
25. L. Wang, H. Li, X. Huang, E. Baudrin, *Solid State Ionics,* 193 (2011) 32.
26. H. Lee, P. Muralidharan, C.M. Mari, R. Ruffo, D.K. Kim, *J. Power Sources,* 196 (2011) 10712.
27. S. Patoux, L. Daniel, C. Bourbon, H. Lignier, C. Pagano, F. Le Cras, S. Jouanneau, S. Martinet, *J. Power Sources,* 189 (2009) 344.
28. F.G.B. Ooms, E.M. Kelder, J. Schoonman, M. Wagemaker, F.M. Mulder, *Solid State Ionics,* 152-153 (2002) 143.
29. U. Lafont, C. Locati, W.J.H. Borghols, A. Łasin´ska, J. Dygas, A.V. Chadwick, E.M. Kelder, *J. Power Sources,* 189 (2009) 179.

30. Y. Yao, H. Liu, G. Li, H. Peng, K. Chen, *Mater. Chem. Phys.*, 143 (2014) 867.
31. W.W. Wu, H.F. Xiang, G.B. Zhong, W. Suc, W. Tang, Y. Zhang, Y. Yu, C.H. Chen, *Electrochim. Acta*, 119 (2014) 206.
32. S. Myung, S. Komaba, N. Kumagai, H. Yashiro, H. Chung, T.g Cho, *Electrochim. Acta*, 47 (2002) 2543.
33. R.S. Nicholson, *Anal. Chem.*, 37 (1965) 1351.
34. Y. Xia, H. Takeshige, H. Noguchi and M. Yoshio, *J. Power Sources*, 56(1995) 61.
35. T. Yang, N. Zhang, Y. Lang and K. Sun, *Electrochim. Acta*, 56(2011) 4058.
36. X. Zhang, F. Cheng, K. Zhang, Y. Liang, S. Yang, J. Liang, J. Chen, *RSC Adv.*, 2(2012) 5669.
37. J. Liu, A. Manthiram, *J. Phys. Chem. C*, 113(2009) 15073.
38. M. Kunduraci, G.G. Amatucci, *Electrochim. Acta*, 53(2008) 4193.
39. M.W. Xiang, C.W. Su, L.L. Feng, M.L. Yuan, J.M. Guo, *Electrochim. Acta*, 125 (2014) 524.
40. G.Y. Liu, Y.N. Li, B.S. Wang, *Int. J. Electrochem. Sci.*, 10 (2015) 3124.
41. Y.Z. Wang, X. Shao, H.Y. Xu, M. Xie, S.X. Deng, H. Wang, J.B. Liu, H. Yan, *J. Power Sources*, 226 (2013) 140.
42. M. Aklalouch, R.M. Rojas, J.M. Rojo, I. Saadoune, J.M. Amarilla, *Electrochim. Acta*, 54 (2009) 7542.
43. L.J. Xi, H.E. Wang, Z.G. Lu, S.L. Yang, R.G. Ma, J.Q. Deng, C.Y. Chung, *J. Power Sources*, 198 (2012) 251.
44. J.J. Shiu, W.K. Pang, S.g Wu, *J. Power Sources*, 244 (2013) 35.